

Fine-Tuning a Simulation-Driven Estimator

Braghadeesh Lakshminarayanan, Margarita A. Guerrero, Cristian R. Rojas

Abstract—Many industries now deploy high-fidelity simulators (digital twins) to represent physical systems, yet their parameters must be calibrated to match the true system. This motivated the construction of simulation-driven parameter estimators, built by generating synthetic observations for sampled parameter values and learning a supervised mapping from observations to parameters. However, when the true parameters lie outside the sampled range, predictions suffer from an out-of-distribution (OOD) error. This paper introduces a fine-tuning approach for the Two-Stage estimator that mitigates OOD effects and improves accuracy. The effectiveness of the proposed method is verified through numerical simulations.

Index Terms—Estimation, Identification, Two-Stage Estimator, Machine Learning.

I. INTRODUCTION

Recent advances in high-fidelity simulation have popularized digital twins (DTs)—software replicas of physical systems that let engineers explore operating conditions safely and cheaply before deployment [8], [9], [15]. In practice, once a DT is engineered, most modeling choices are fixed; what remains is calibrating a small set of parameters so the DT replicates a specific physical system.

When a DT is available, one can generate synthetic input–output data [14] over a range of parameter settings and train a supervised machine learning model that maps observations to these settings, thereby yielding a *simulation-driven estimator*. At implementation, this simulation-driven estimator takes real measurements and returns parameter estimates [2], [5], [6]. The Two-Stage (TS) estimator [4], [5] is an attractive simulation-driven estimator with a simple structure that involves two stages: (i) first, the observations are compressed into representative features, and then (ii) these compressed features, along with their corresponding parameter values, are used to train a supervised machine learning model. This structure avoids the need for an explicit likelihood function and it requires low computation time for producing estimates, due to extensive offline training, compared to standard point estimators like the prediction error method (PEM) and the dual Extended Kalman Filter (dual-EKF) [10, App. B.2]. The TS estimator can also be used to learn control design rules, effectively taking the *human out of the loop* [1].

A limitation of TS is prior-range misspecification: when the parameters of the true system lie outside the range

of the synthetic parameter values used during training, the accuracy of the pretrained TS estimator can be low; this is called an out-of-distribution (OOD) case. In this paper, we tackle this issue by fine-tuning only the second stage of TS, implemented as a multi-head neural network for its end-to-end differentiability, using the DT and the new observations.

Our novel fine-tuning procedure first compares the compressed features from real data to those produced by the DT at the TS initial prediction, to determine whether an OOD case has occurred by applying a statistical test based on a whitened feature discrepancy measure constructed from estimated feature covariances. If an OOD case is detected, we: (i) compute Gauss–Newton (GN) iterations on the initial prediction by TS, (ii) generate a confidence set around the GN update and re-simulate a targeted local training dataset with the DT, and (iii) fine-tune the final portion of the second stage of the TS estimator, which is inspired from *transfer learning* [13] approaches to system identification [3], [12]. In particular, our contributions are the following:

- We derive a feature-space OOD test based on DT-derived feature statistics and whitening;
- we propose a label-free fine-tuning approach that combines Gauss–Newton iterations with a confidence set to generate a fresh synthetic dataset for the retraining of TS;
- we design a minimal update of the second-stage of TS, adjusting only its final layers; and
- we numerically validate our proposed approach against standard baselines.

The remainder of the paper is organized as follows. In Section II, we introduce the problem statement. In Section III, our method for fine-tuning the pretrained TS estimator is detailed, and in Section IV, we demonstrate the effectiveness of our approach through several numerical examples. Finally, Section V concludes the paper.

II. PROBLEM STATEMENT

We consider a data-generating mechanism $\mathcal{M}(\theta)$ —a high-fidelity simulator or digital twin (DT)—parameterized by $\theta \in \Theta \subseteq \mathbb{R}^d$. For notational simplicity, we assume a single-input single-output (SISO) setting: given an N -length *scalar* input sequence $\mathbf{u} = (u_1, \dots, u_N)^\top \in \mathbb{R}^N$, the DT produces a (possibly stochastic) *scalar* output sequence $\mathbf{y} = (y_1, \dots, y_N)^\top \in \mathbb{R}^N$. Concretely, $\mathbf{y} = \mathbf{y}(\theta; \omega)$, where ω denotes the simulator’s noise seed (or any internal randomness). Assume that a length- N trajectory $\mathbf{z}_0 = (u_1, y_{0,1}, \dots, u_N, y_{0,N}) \in \mathbb{R}^{2N}$ has been measured from the DT at some unknown parameter $\theta_0 \in \Theta$. The goal is

This work has been partially supported by the Swedish Research Council under contract number 2023-05170, and by the Wallenberg AI, Autonomous Systems and Software Program (WASP) funded by the Knut and Alice Wallenberg Foundation. The authors are with the Division of Decision and Control Systems, KTH Royal Institute of Technology, 100 44 Stockholm, Sweden (e-mails: blak@kth.se; mags3@kth.se; ccro@kth.se).

to estimate θ_0 from \mathbf{z}_0 by constructing a *simulation-driven parameter estimator*.

Given a *calibration set* $\Theta_p \subseteq \Theta$, constructed from prior domain knowledge and anticipated operating regimes, we draw i.i.d. parameter settings $\{\tilde{\theta}_i\}_{i=1}^m$ from Θ_p . For each draw $\tilde{\theta}_i$, we run the simulator with (possibly) its own noise seed ω_i and the chosen input sequence¹ \mathbf{u} , obtaining $\mathbf{z}_i = (u_1, y_{i,1}, \dots, u_N, y_{i,N})$. This yields a synthetic, labeled dataset $\mathcal{D} = \{(\mathbf{z}_i, \tilde{\theta}_i)\}_{i=1}^m$. An estimator $\hat{\theta}_{\text{pre}}: \mathbb{R}^{2N} \rightarrow \mathbb{R}^d$ is then fitted by solving the following minimization problem over a prescribed function class \mathcal{F} (e.g. a neural network):

$$\hat{\theta}_{\text{pre}}(\cdot) \in \arg \min_{F \in \mathcal{F}} \frac{1}{m} \sum_{i=1}^m L(F(\mathbf{z}_i), \tilde{\theta}_i), \quad (1)$$

where $L: \mathbb{R} \times \mathbb{R} \rightarrow \mathbb{R}_{\geq 0}$ is a scalar loss (e.g., squared or Huber). Following Eq. (1), an estimate of θ_0 is obtained as

$$\hat{\theta}_0 = \hat{\theta}_{\text{pre}}(\mathbf{z}_0), \quad (2)$$

where \mathbf{z}_0 are the observations (input-output data) collected from the system $\mathcal{M}(\theta_0)$.

When $\theta_0 \in \Theta_p$, suitable choices of \mathcal{F} and L can lead to an accurate estimate $\hat{\theta}_{\text{pre}}(\mathbf{z}_0)$ of θ_0 . However, because Θ_p is user-specified and may omit plausible regimes, an *out-of-distribution (OOD)* situation may occur if $\theta_0 \notin \Theta_p$, or if there are not enough samples $\tilde{\theta}_i$ in the neighborhood of θ_0 . Hence, performance can degrade under an OOD, motivating mechanisms that refine $\hat{\theta}_{\text{pre}}(\cdot)$ at implementation phase. In this paper, we focus on a special class of simulation-driven estimators $\hat{\theta}_{\text{pre}}(\cdot)$, known as the Two-Stage (TS) estimator.

A. The Two-Stage (TS) Estimator

The TS estimator [4], [5] decomposes (1) into two-stages: a fixed *compression* of \mathbf{z} into low-dimensional features, followed by a supervised machine learning model that map these features to the parameters.

A.1 Stage 1 (Compression)

Choose a deterministic feature map

$$h: \mathbb{R}^{2N} \rightarrow \mathbb{R}^n, \quad n \ll 2N, \quad (3)$$

e.g., the estimated coefficients of an AR/ARX/ARMAX model fitted to the data. Let $\mathbf{x}_i = h(\mathbf{z}_i)$ and form the synthetic dataset

$$\mathcal{D}_{\text{tr}} = \{(\mathbf{x}_i, \tilde{\theta}_i)\}_{i=1}^m = \{(h(\mathbf{z}_i), \tilde{\theta}_i)\}_{i=1}^m \subset \mathbb{R}^n \times \mathbb{R}^d. \quad (4)$$

A.2. Stage 2 (Supervised mapping)

Let $\mathbf{x} = h(\mathbf{z}) \in \mathbb{R}^n$ be the Stage-1 feature vector. The Stage-2 function $g_{\text{pre}}: \mathbb{R}^n \rightarrow \mathbb{R}^d$ is a fully connected deep neural network with *trunk* and *head* layers.

A.2.1 Trunk Layers

The trunk of the second stage neural network is mathematically described as follows: Let $\mathbf{s}^{(0)} = \mathbf{x}$ be the input layer and for $r = 1, \dots, R-1$, the output of the r^{th} hidden

layer is given by $\mathbf{s}^{(r)} = \sigma_r(\mathbf{W}_r \mathbf{s}^{(r-1)})$, $\mathbf{W}_r \in \mathbb{R}^{p_r \times p_{r-1}}$, where \mathbf{W}_r denotes the weights of the hidden layer r , $\sigma_r(\cdot)$ denotes an activation function (e.g. ReLU(\cdot)), $p_0 = n$ and $p_{R-1} = p$. These R layers constitute the *trunk* of g_{pre} . The trunk output is $\mathbf{t}(\mathbf{x}) := \mathbf{s}^{(R-1)} \in \mathbb{R}^p$ and its parameters are $\phi := \{\mathbf{W}_r\}_{r=1}^{R-1}$.

A.2.2 Head Layers

To finally predict the targets $\tilde{\theta}_i \in \Theta_p \subseteq \mathbb{R}^d$, which can be multidimensional ($d > 1$), we append $V-1$ subsequent hidden layers for each parameter dimension, and these $V-1$ layers corresponding to each individual parameter constitute the *head* of $g_{\text{pre}}(\cdot)$, denoted as $\mathbf{h}_j^{(v)}$, where $v = 1, \dots, V-1$. We additionally impose that the weights of the first of these $V-1$ layers are least correlated, which is needed to ensure that each parameter is correctly identified. We precisely formalize the structure of the head as the following:

For each parameter index $j \in \{1, \dots, d\}$, starting from $\mathbf{h}_j^{(0)} = \mathbf{t}(\mathbf{x})$ and for $v = 1, \dots, V-1$ define

$$\mathbf{h}_j^{(v)} = \sigma_{j,v}(\mathbf{U}_{j,v} \mathbf{h}_j^{(v-1)}), \quad \mathbf{U}_{j,v} \in \mathbb{R}^{q_{j,v} \times q_{j,v-1}}, \quad (5)$$

where $\mathbf{U}_{j,v}$ corresponds to the weights of hidden layer v of head j , and $\sigma_{j,v}(\cdot)$ corresponds to the activation function of v^{th} hidden layer of head j , with $q_{j,0} = p$. The scalar output for head j is linear:

$$\hat{\theta}_j(\mathbf{x}) = \mathbf{a}_j^\top \mathbf{h}_j^{(V-1)}, \quad \mathbf{a}_j \in \mathbb{R}^{q_{j,V-1}}. \quad (6)$$

The head parameters are then defined as $\psi_j := \{(\mathbf{U}_{j,v})_{v=1}^{V-1}, \mathbf{a}_j\}$, and $\Psi := (\psi_1, \dots, \psi_d)$. Stacking the d heads yields the second stage output as

$$g_{\text{pre}}(\mathbf{x}; \phi, \Psi) := \begin{bmatrix} \hat{\theta}_1(\mathbf{x}) \\ \vdots \\ \hat{\theta}_d(\mathbf{x}) \end{bmatrix} \in \mathbb{R}^d, \quad [g_{\text{pre}}(\mathbf{x}; \phi, \Psi)]_j := \hat{\theta}_j(\mathbf{x}). \quad (7)$$

Given the training dataset $\mathcal{D}_{\text{tr}} = \{(\mathbf{x}_i, \tilde{\theta}_i)\}_{i=1}^m$, we learn (ϕ, Ψ) by solving the following optimization problem via stochastic gradient descent:

$$\begin{aligned} (\hat{\phi}, \hat{\Psi}) \in \arg \min_{\phi, \Psi} \frac{1}{m} \sum_{i=1}^m \sum_{j=1}^d \tilde{w}_j L(\hat{\theta}_j(\mathbf{x}_i), [\tilde{\theta}_i]_j) \\ + \lambda_{\text{orth}} \sum_{1 \leq j < k \leq d} \|\mathbf{U}_{j,1} \mathbf{U}_{k,1}^\top\|_F^2, \end{aligned} \quad (8)$$

where $\tilde{w}_j \geq 0$ are per-parameter weights, $[\tilde{\theta}_i]_j$ denotes the j^{th} coordinate of $\tilde{\theta}_i$, $\lambda_{\text{orth}} \geq 0$ is a regularization coefficient, and the last term encourages diversity among the heads by penalizing the correlations between their first-layer weights.

The final TS estimator is the composition $\hat{\theta}_{\text{pre}}(\mathbf{z}) = g_{\text{pre}}(h(\mathbf{z}); \hat{\phi}, \hat{\Psi}) \in \mathbb{R}^d$. At implementation phase, given a new trajectory \mathbf{z}_0 generated by $\mathcal{M}(\theta_0)$, the point estimate is

$$\hat{\theta}_0 = \hat{\theta}_{\text{pre}}(\mathbf{z}_0) = g_{\text{pre}}(h(\mathbf{z}_0); \hat{\phi}, \hat{\Psi}). \quad (9)$$

If $\theta_0 \notin \Theta_p$, then (\mathbf{z}_0, θ_0) is OOD w.r.t. \mathcal{D}_{tr} , and (9) may yield a poor estimate of θ_0 . We shall now state a fine-tuning approach to overcome this problem.

¹Due to space limitations, in this paper the input sequence is considered fixed, even though the treatment can be extended to random inputs.

III. FINE-TUNING THE TS ESTIMATOR

We propose a *simulation-driven transfer learning* procedure to improve a pretrained TS estimator when faced with out-of-distribution (OOD) observations. The key idea is to keep the first stage feature extractor h unchanged and to *fine-tune only the last layers* of the second stage $g_{\text{pre}}(\cdot; \phi, \Psi)$. Concretely, we *freeze* the parameters ϕ learned during pretraining and *update* only the remaining parameters Ψ using a small, targeted synthetic dataset produced by the DT in a neighborhood of the current TS estimate. This follows standard transfer-learning practice—earlier layers capture generic structure and are preserved; only the final layers are tuned [20].

Because fine-tuning adds computation and is unnecessary for in-distribution data, we first perform a *feature-space statistical test* to decide whether an OOD has occurred. If an OOD is detected, we (i) *align* the simulator’s features to the observed ones via a few Gauss–Newton (GN) steps around the initial TS estimate, and then (ii) use the geometry described by the Fisher information matrix at that estimate to sample an informative cloud of nearby parameters. By using the DT to generate more synthetic data for these samples, we obtain labeled feature–parameter pairs concentrated near the operating point. Finally, we *retrain only the final layers* of g_{pre} on this targeted synthetic dataset, keeping ϕ fixed (cf. (8)). In summary, the transfer learning approach to fine tune TS consists of the following three steps:

- **Step 1 — Feature-space OOD detector.** Test whether the observed features $\mathbf{x}_{\text{obs}} := h(\mathbf{z}_0)$ are statistically consistent with features generated by the simulator at the initial TS prediction $\hat{\theta}_{\text{init}} = g_{\text{pre}}(h(\mathbf{z}_0); \hat{\phi}, \hat{\Psi})$. If consistent, skip fine-tuning and deploy $\hat{\theta}_{\text{pre}}(\cdot)$.
- **Step 2 — Synthetic data generation.** If an OOD is detected, perform a few GN iterations in feature space (regularized toward $\hat{\theta}_{\text{init}}$) to obtain an improved estimate $\hat{\theta}_{\text{GN}}$. Then, derive a confidence region around $\hat{\theta}_{\text{GN}}$; sample an informative cloud of parameters from this region; and simulate the DT at these samples to form a small synthetic dataset of feature–parameter pairs.
- **Step 3 — Final-layer transfer.** With ϕ frozen, update only Ψ on the small synthetic dataset using a weighted loss (e.g., weighted least squares or Huber). The result is an improved estimator $g_{\text{pre}}(\cdot; \hat{\phi}, \hat{\Psi})$ under the OOD.

A. Step 1: Feature–Space OOD Detector

We now provide a procedure to detect an OOD scenario. To this end, we appeal to a bootstrapped version of Wald’s test [16], [18], [7]. The null hypothesis, H_0 , is that the observed features, \mathbf{x}_{obs} , are statistically consistent with the features generated by the simulator when its parameter is set to the initial estimate, $\hat{\theta}_{\text{init}} := g_{\text{pre}}(\mathbf{x}_{\text{obs}}; \hat{\phi}, \hat{\Psi})$.

The procedure begins by computing the initial parameter estimate from the new observations, \mathbf{z}_0 , generated by the system $\mathcal{M}(\theta_0)$, where θ_0 is unknown. This is done by first extracting its features, $\mathbf{x}_{\text{obs}} := h(\mathbf{z}_0)$, and then applying the

pre-trained second-stage estimator, outputting initial estimate of θ_0 as $\hat{\theta}_{\text{init}} := g_{\text{pre}}(\mathbf{x}_{\text{obs}}; \hat{\phi}, \hat{\Psi})$. Next, we fix the simulator’s parameter at $\hat{\theta}_{\text{init}}$ and run K simulations, each with a different random seed ω_k . Applying the feature extractor $h(\cdot)$ to each of the K resulting trajectories yields a $K \times n$ matrix of simulated features: $\mathbf{H} := ((\mathbf{x}^{(1)})^\top, \dots, (\mathbf{x}^{(K)})^\top)^\top$, where $\mathbf{x}^{(j)} = h(\mathbf{z}_j)$, and \mathbf{z}_j is the input-output trajectory generated by the simulator $\mathcal{M}(\hat{\theta}_{\text{init}})$ at the noise seed ω_j . This matrix, \mathbf{H} , characterizes the expected variability of the features if the true parameter were indeed $\hat{\theta}_{\text{init}}$. To construct a test statistic, we compute a whitened discrepancy measure. From the simulated features \mathbf{H} , we first estimate the feature mean $\boldsymbol{\mu}_h$ and the regularized covariance \mathbf{S}_h :

$$\begin{aligned} \boldsymbol{\mu}_h &:= \frac{1}{K} \sum_{k=1}^K \mathbf{H}_{k:}^\top, \\ \mathbf{S}_h &:= \frac{1}{K-1} \sum_{k=1}^K [\mathbf{x}^{(k)} - \boldsymbol{\mu}_h][\mathbf{x}^{(k)} - \boldsymbol{\mu}_h]^\top \\ &\quad + \varepsilon \mathbf{I}_n, \quad \varepsilon > 0, \end{aligned}$$

where $\mathbf{H}_{k:} = (\mathbf{x}^{(k)})^\top$, and \mathbf{I}_n is an $n \times n$ identity matrix. The covariance matrix is then used to define a whitening transform, $\mathbf{W} := \mathbf{S}_h^{-1/2}$, which normalizes the feature space by accounting for correlations and different scales among the features. The test statistic for our observed data is the whitened squared residual norm:

$$s_{\text{obs}} = \|\mathbf{W}(\mathbf{x}_{\text{obs}} - \boldsymbol{\mu}_h)\|_2^2. \quad (10)$$

Finally, we establish a critical value for this statistic using the bootstrap principle. We compute the same whitened statistic for each of the K simulated feature vectors:

$$s_k = \|\mathbf{W}(\mathbf{H}_{k:}^\top - \boldsymbol{\mu}_h)\|_2^2, \quad k = 1, \dots, K. \quad (11)$$

The set $\{s_k\}_{k=1}^K$ provides an empirical distribution of the test statistic under H_0 . We define our decision threshold, $q_{1-\alpha}$, as the empirical $(1 - \alpha)$ -quantile of this distribution.

Decision rule: If $s_{\text{obs}} > q_{1-\alpha}$, we reject the null hypothesis H_0 , conclude that an OOD scenario is likely, and proceed to Step 2. Otherwise, the observation is deemed statistically consistent with the variability at $\hat{\theta}_{\text{init}}$, and we retain the pretrained estimator without fine-tuning.

B. Step 2: Synthetic data generation

If $s_{\text{obs}} > q_{1-\alpha}$, then the compressed features from the first-stage of TS evaluated at $\hat{\theta}_{\text{init}}$ fail to explain \mathbf{x}_{obs} in the whitened space. In that case, we refine $\hat{\theta}_{\text{init}}$ by running Gauss–Newton (GN) iterations that minimize the whitened feature residual between the observed feature and the first-stage-generated feature. Because this residual is random, the Gauss–Newton estimate, denoted $\hat{\theta}_{\text{GN}}$, still carries parameter uncertainty. To effectively fine-tune the second stage of the TS estimator, we need to generate a cloud of synthetic data that covers the region of plausible parameter values around this estimate. We shall now describe precisely the synthetic dataset generation for fine-tuning the second stage of TS as follows.

a) *Gauss–Newton update*: We compute the GN update starting from the TS initial estimate. Define a seed-averaged simulator feature map over a small seed set \mathcal{S}_{avg} :

$$\begin{aligned}\bar{\mathbf{f}}(\boldsymbol{\theta}) &:= \frac{1}{K_{\text{avg}}} \sum_{\omega \in \mathcal{S}_{\text{avg}}} h(\mathbf{z}(\boldsymbol{\theta}, \omega; \mathbf{u})), \\ \mathbf{r}(\boldsymbol{\theta}) &:= \mathbf{W}(\bar{\mathbf{f}}(\boldsymbol{\theta}) - \mathbf{x}_{\text{obs}}) \in \mathbb{R}^n,\end{aligned}\quad (12)$$

where $\mathbf{z}(\boldsymbol{\theta}, \omega; \mathbf{u})$ is the input-output trajectory generated by the simulator for a specific parameter vector $\boldsymbol{\theta}$, a random seed ω , and fixed inputs \mathbf{u} . Let $\mathbf{J}(\boldsymbol{\theta}) := \partial \bar{\mathbf{f}}(\boldsymbol{\theta}) / \partial \boldsymbol{\theta} \in \mathbb{R}^{n \times d}$ and $\mathbf{J}_w(\boldsymbol{\theta}) := \mathbf{W} \mathbf{J}(\boldsymbol{\theta})$. A first-order Taylor expansion gives $\mathbf{r}(\boldsymbol{\theta} + \boldsymbol{\delta}) \approx \mathbf{r}(\boldsymbol{\theta}) + \mathbf{J}_w(\boldsymbol{\theta}) \boldsymbol{\delta}$. We minimize the regularized objective

$$v(\boldsymbol{\theta}) = \frac{1}{2} \|\mathbf{r}(\boldsymbol{\theta})\|_2^2 + \frac{\gamma}{2} \|\boldsymbol{\theta} - \hat{\boldsymbol{\theta}}_{\text{init}}\|_2^2, \quad \gamma > 0, \quad (13)$$

whose quadratic approximation yields the normal equations

$$\underbrace{(\mathbf{J}_w^\top \mathbf{J}_w + \gamma \mathbf{I}_d)}_{=: \mathbf{G}_\gamma} \boldsymbol{\delta} = -(\mathbf{J}_w^\top \mathbf{r}(\boldsymbol{\theta}) + \gamma(\boldsymbol{\theta} - \hat{\boldsymbol{\theta}}_{\text{init}})), \quad (14)$$

and the regularized GN step

$$\boldsymbol{\delta}^* = -\mathbf{G}_\gamma^{-1} (\mathbf{J}_w^\top \mathbf{r}(\boldsymbol{\theta}) + \gamma(\boldsymbol{\theta} - \hat{\boldsymbol{\theta}}_{\text{init}})), \quad (15)$$

followed by a backtracking line search (e.g., Armijo). A few iterations yield $\hat{\boldsymbol{\theta}}_{\text{GN}}$.

b) *Sampling procedure*: $\hat{\boldsymbol{\theta}}_{\text{GN}}$ is a point estimate derived from a single, noisy observation and is therefore uncertain. To effectively fine-tune the TS estimator, we must generate a cloud of synthetic data that explores the region of plausible parameter values around this estimate. We employ a hybrid sampling strategy that combines a *confidence-ellipsoid* based method with an alternative sampling scheme.

Our primary approach is to sample from the approximate $1 - \beta$ confidence ellipsoid for the true parameter $\boldsymbol{\theta}_0$. This region is defined by the set of all $\boldsymbol{\theta}$ satisfying:

$$(\boldsymbol{\theta} - \hat{\boldsymbol{\theta}}_{\text{GN}})^\top \mathbf{G}(\boldsymbol{\theta} - \hat{\boldsymbol{\theta}}_{\text{GN}}) \leq \chi_d^2(\beta), \quad (16)$$

where $\chi_d^2(\beta)$ is the chi-squared quantile and $\mathbf{G} \approx \mathbf{J}_w^\top \mathbf{J}_w + \lambda \mathbf{I}_d$ is the approximate Fisher Information Matrix (FIM). This ellipsoid represents a high-confidence region, and sampling from it is statistically efficient for exploring well-identified parameters. However, this primary method can fail if the model is insensitive to one or more parameters. In such cases, the FIM, \mathbf{G} , becomes ill-conditioned, causing the confidence ellipsoid to be stretched along the insensitive directions, and thereby making the sampling procedure numerically unstable. To overcome this, we alternate between this sampling approach and *sensitivity* sampling. The latter sampling procedure handles the ill-conditioned directions. It works by generating samples along individual parameter axis with a step size that is inversely proportional to the simulator’s sensitivity to that parameter. The sensitivity of coordinate j is defined as $s'_j := \|\mathbf{J}_w \mathbf{e}_j\|_2$. To set the sampling scale, we define two quantities. First, $\Delta_{\text{misfit}} := \|\mathbf{r}(\hat{\boldsymbol{\theta}}_{\text{GN}})\|_2$, measures the discrepancy between the observed summary statistic and the one generated by the simulator at the point estimate $\hat{\boldsymbol{\theta}}_{\text{GN}}$. Second, we compute $d_{\text{med}} :=$

$\text{median}_k d_k$, based on the spread of pre-computed summary features, where each $d_k := \|\mathbf{W}(\mathbf{H}_k - \boldsymbol{\mu}_h)\|_2$ represents the whitened residual. We then set coordinate scales, r_j , that increase exploration for less sensitive parameters (small s'_j) while also adapting to the simulator’s noise level and the current feature mismatch as

$$r_j = \frac{d_{\text{med}}}{s'_j} \Delta_{\text{misfit}}. \quad (17)$$

Our final sampling procedure combines confidence ellipsoid and sensitivity sampling, yielding a hybrid sampling scheme, given by $\boldsymbol{\theta}_k = \hat{\boldsymbol{\theta}}_{\text{GN}} + \Delta \boldsymbol{\theta}_k$, where $\Delta \boldsymbol{\theta}_k$ is drawn as

$$\begin{aligned}(\text{confidence set sampling}) \quad \Delta \boldsymbol{\theta}_k &= \mathbf{L} \mathbf{z}, \quad \mathbf{z} \sim \mathcal{N}(\mathbf{0}, \mathbf{I}_d), \\ &\quad \mathbf{L} \mathbf{L}^\top \approx \mathbf{G}^{-1}, \\ (\text{sensitivity sampling}) \text{ pick } i &\sim \text{Unif}\{1, \dots, d\}, \quad \zeta \sim \mathcal{N}(0, r_i^2), \\ \Delta \boldsymbol{\theta}_k &= \zeta \mathbf{e}_i,\end{aligned}\quad (18)$$

where $\mathbf{e}_i \in \mathbb{R}^d$ is the i -th standard basis vector (1 at position i , zeros elsewhere), and \mathbf{L} is the Cholesky factor of \mathbf{G}^{-1} . To create the fine-tuning dataset, $\mathcal{D}_{\text{fine}}$, we generate a synthetic observation $\bar{\mathbf{z}}_k$ from the simulator for each parameter sample $\boldsymbol{\theta}_k$. Each observation is then compressed using $h(\cdot)$, forming a dataset of pairs: $\mathcal{D}_{\text{fine}} = \{(h(\bar{\mathbf{z}}_k), \boldsymbol{\theta}_k)\}_{k=1}^{M_{\text{FT}}}$.

Remark 3.1: The quantity Δ_{misfit} can be artificially small due to noise induced by the randomness of the simulator \mathcal{M} , so the naive radius $\Delta_{\text{misfit}}/s'_j$ would under-explore. Multiplying by $d_{\text{med}} := \text{median}_k \|\mathbf{W}(\mathbf{H}_k - \boldsymbol{\mu}_h)\|_2$ rescales the step to the *typical* feature fluctuation at $\boldsymbol{\theta}_{\text{init}}$, giving $r_j = (d_{\text{med}}/s'_j) \Delta_{\text{misfit}}$. This preserves the desired inverse-sensitivity ($1/s'_j$) while making the samples noise-aware.

C. Step 3: Final-Layer Transfer on a Targeted Set

Finally, we freeze the early layers of $g_{\text{pre}}(\cdot; \boldsymbol{\phi}, \boldsymbol{\Psi})$ (i.e., keep $\boldsymbol{\phi}$ fixed) and modify only the last layers, yielding $g_{\text{ft}}(\cdot; \boldsymbol{\phi}, \boldsymbol{\Psi}_{\text{ft}})$. We fit $\boldsymbol{\Psi}$ on $\mathcal{D}_{\text{fine}}$ with a small number of gradient steps using a weighted objective (cf. (8)):

$$\begin{aligned}\min_{\boldsymbol{\Psi}} \frac{1}{M_{\text{FT}}} \sum_{m=1}^{M_{\text{FT}}} \sum_{j=1}^d \tilde{w}_j L\left(\left[g_{\text{pre}}(h(\bar{\mathbf{z}}_m); \boldsymbol{\phi}, \boldsymbol{\Psi}) \right]_j, [\bar{\boldsymbol{\theta}}_m]_j \right) \\ + \lambda_{\text{orth}} \sum_{1 \leq j < k \leq d} \|\mathbf{U}_{j,1} \mathbf{U}_{k,1}^\top\|_F^2.\end{aligned}\quad (19)$$

IV. SIMULATION STUDY

We evaluate the proposed fine-tuning scheme on two nonlinear systems: (i) the Van der Pol (VDP) oscillator and (ii) cascaded water tanks. In both cases, the model structure is known but the true parameters may lie outside the sampling set used to pretrain the TS estimator. We compare against **TS-pre** (pretrained TS), the **Prediction Error Method** (PEM) [11], and a **dual Extended Kalman Filter** [17] (dual-EKF). For PEM and dual-EKF we report results under three initializations: *Good Init* (a Gaussian perturbation of the true parameter value), *TS-Init* (initialized at $\hat{\boldsymbol{\theta}}_{\text{pre}}(\mathbf{z}_0)$), and *Bad/Worse-Case Init* (point far from $\boldsymbol{\theta}_0$).

a) *Common settings:* For all simulations we set $K = 150$ in (10). The whitened Jacobian \mathbf{J}_w is obtained via finite differences. To compute $\mathbf{f}(\theta)$ in (12) and the Jacobians, we use common random numbers with the seed set $S_{\text{avg}} = \{8000, 8001, 8002\}$. Both examples are simulated in discrete time using forward Euler with a fixed step size Δt (VDP: 0.05 s; tanks: 0.5 s). The Gauss–Newton regularization parameter in (13) is $\gamma = 10^{-3}$ (VDP) and $\gamma = 10^{-4}$ (tanks). The orthogonality regularizer λ_{orth} on the first head layer is 0 for VDP (single output) and 5×10^{-4} for the tanks.

b) *Feature compression and stage-2 network.:* For VDP we use AR(5) coefficients fitted to y ; for the tanks we use ARX(32, 32) coefficients fitted to (y, u) . The stage-2 regressor g_{pre} is a fully connected network with a shared trunk and one head per parameter, and the following settings:

- **VDP:** trunk (256, 128) with ReLU+Dropout(0.1); one head (depth 2, hidden 128, Tanh+Dropout(0.1)). Adam with lr 10^{-3} , batch size 64, 200 epochs. Offline bank size $m = 10000$; fine-tune cloud $M_{\text{FT}} = 400$.
- **Tanks:** trunk (256, 256) with LayerNorm+LeakyReLU+Dropout(0.15); four heads (depth 3, hidden 64, LayerNorm+Tanh+Dropout(0.15)). Adam with lr 10^{-3} , batch size 64, 250 epochs. Offline bank size $m = 10000$; fine-tune cloud $M_{\text{FT}} = 1000$.

In the fine-tuned TS estimator (TS-fine), we freeze the trunk and retrain only the head layers on the synthetic cloud around the GN update; for the tanks we also use a smaller head (hidden 64, depth 1, dropout 0.20) with early stopping.

A. Van der Pol Oscillator

The VDP dynamics are

$$\dot{x}_1 = x_2, \quad \dot{x}_2 = \mu(1 - x_1^2)x_2 - x_1 + w_k, \quad y = x_1, \quad (20)$$

with unknown $\mu > 0$ and small process noise $w_k \sim \mathcal{N}(0, 0.02)$. We collect $N = 300$ length observations for each $\mu_i \sim \text{Unif}[0, 2.5]$ to form the offline training set \mathcal{D}_{tr} .

OOD tests. We evaluate at $\mu = 3.0$ and $\mu = 5.0$, which are outside the pretraining range. Over $n_{\text{mc}} = 100$ Monte-Carlo runs, we report mean squared errors (MSEs) and average trajectories of the true system (20) and of each method (Figs. 1–2). TS-fine has a substantially smaller MSE than TS-pre and outperforms dual-EKF/PEM under poor initializations; PEM with a good initialization can perform well, but is initialization-sensitive, unlike TS-fine.

1) *Remark on choosing α :* We sweep $\alpha \in \{0.50, 0.30, 0.20, 0.10, 0.05, 0.01\}$ on two scenarios ($N = 300$, $n_{\text{mc}} = 100$ trials): (i) in-distribution (ID, $\mu = 1.5$) and (ii) out-of-distribution (OOD, $\mu = 4.5$). Empirically, for ID the OOD detection rate drops to 0 by $\alpha = 0.05$ and TS-fine offers no benefit in terms of MSE, whereas for OOD the statistical test is positive essentially always and fine-tuning reduces the MSE by orders of magnitude (e.g., $4.70 \rightarrow 5 \times 10^{-3}$). Thus choosing $\alpha \in [0.05, 0.10]$ avoids unnecessary fine-tuning on ID while reliably detecting OOD cases.

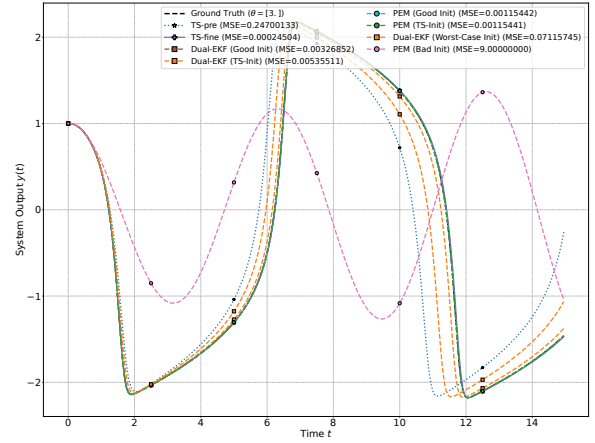


Fig. 1: VDP (OOD $\mu = 3.0$): ground-truth vs. mean predictions over 100 MC runs. The trajectory plots are measurements without noise.

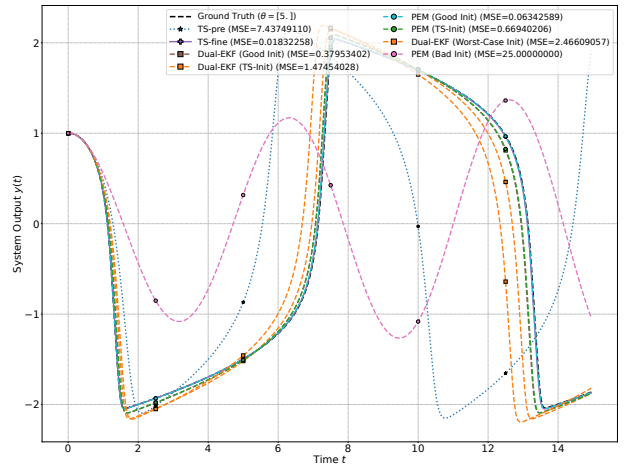


Fig. 2: VDP (OOD $\mu = 5.0$): ground-truth vs. mean predictions over 100 MC runs. The trajectory plots are measurements without noise.

B. Cascaded Water Tanks

The cascaded water tanks dynamics are given by

$$\begin{aligned} \dot{h}_1 &= -k_1 \sqrt{|h_1|} + k_4 u_k + w_k^{(1)}, \\ \dot{h}_2 &= k_2 \sqrt{|h_1|} - k_3 \sqrt{|h_2|} + w_k^{(2)}, \\ y_k &= h_{2,k} + v_k, \end{aligned}$$

with parameter vector $\theta = (k_1, k_2, k_3, k_4)^\top$, process noises $w_k^{(1)}, w_k^{(2)} \stackrel{\text{i.i.d.}}{\sim} \mathcal{N}(0, 0.01)$, and measurement noise $v_k \sim \mathcal{N}(0, 0.02)$. We use $\Delta t = 0.5$ s, and measure y_k as output.

Offline pretraining set. We take samples $\tilde{\theta}_i \sim [0.4, 0.8] \times [0.4, 0.8] \times [0.4, 0.8] \times [0.8, 1.2]$ uniformly ($m = 10000$) and for each $\tilde{\theta}_i$, we collect $N = 400$ length observations. The inputs are PRBS signals [19]: the level of binary signal is drawn i.i.d. from $[0, 3]$ and held for 30 samples.

OOD tests. We consider $\theta = (1.2, 1.2, 0.9, 1.0)^\top$ (OOD 1) and $\theta = (1.3, 1.3, 0.6, 0.7)^\top$ (OOD 2), both outside the pretraining set. For evaluation we fix the same block-uniform

input across runs, simulate with the noise model above, and average over $n_{mc} = 100$ Monte-Carlo (MC) runs. From Fig. 3 and 4, we observe that TS-fine improves upon TS-pre and is competitive with (or better than) dual-EKF/PEM without relying on any initialization. PEM can excel with a good initialization; TS-fine is initialization-free.

a) *Remarks:* (i) The accuracy of TS-pre and TS-fine hinge on the specific first and second-stage choices. In particular, the first-stage compressor should be robust to measurement noise, and our current second stage—an MLP (with LayerNorm for tanks)—can be brittle in low SNR settings. Developing more noise-robust alternatives for both stages is left to future work. (ii) Our aim here is to fine-tune TS, not to optimize the underlying first/second-stage architectures for noise robustness. Consequently, in low SNR regimes, the standard baselines may outperform our current setup.

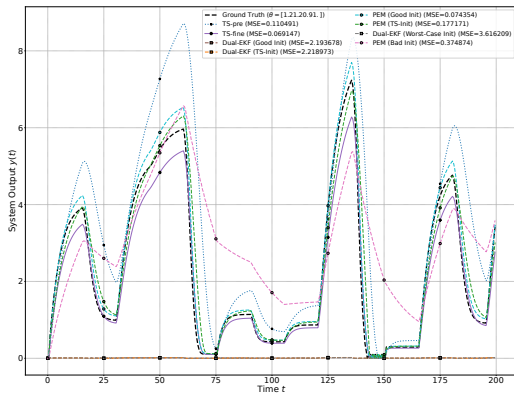


Fig. 3: Tanks (OOD 1): average trajectory (ground truth vs. mean predictions over 100 MC runs. The trajectory plots are measurements without noise.

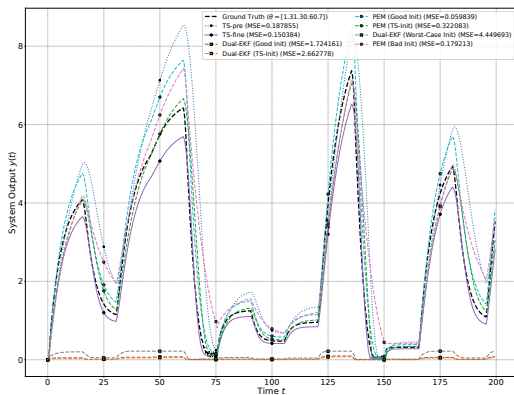


Fig. 4: Tanks (OOD 2): average trajectory (ground truth vs. mean predictions over 100 MC runs. The trajectory plots are measurements without noise.

V. CONCLUSION

In this paper, we have proposed a transfer-learning approach to fine-tune a pretrained, simulation-driven (TS) estimator for out-of-distribution (OOD) scenarios. We first apply a statistical detection test on the compressed features

to flag OOD; if the test detects an OOD, we modify only the second stage (a neural network) by freezing the shared trunk and retraining the last, per-parameter layers using a newly synthesized local dataset. Numerical examples demonstrate that the fine-tuned TS delivers improved performance over the pretrained TS and fares well against initialization-dependent baselines such as dual-EKF and PEM. The main limitation is the computational cost of retraining the heads (and generating the synthetic data); in future work we aim to reduce this overhead.

REFERENCES

- [1] F. Dettù, B. Lakshminarayanan, S. Formentin, and C. R. Rojas. From data to control: a two-stage simulation-based approach. In *Proceedings of the 2024 European Control Conference (ECC)*, pages 3428–3433, 2024.
- [2] T. Diskin, Y. C. Eldar, and A. Wiesel. Learning to estimate without bias. *IEEE Transactions on Signal Processing*, 71:2162–2171, 2023.
- [3] M. Forgione, A. Muni, D. Piga, and M. Gallieri. On the adaptation of recurrent neural networks for system identification. *Automatica*, 155:111092, 2023.
- [4] S. Garatti and S. Bittanti. Estimation of white-box model parameters via artificial data generation: a two-stage approach. *IFAC Proceedings Volumes*, 41(2):11409–11414, 2008.
- [5] S. Garatti and S. Bittanti. A new paradigm for parameter estimation in system modeling. *International Journal of Adaptive Control and Signal Processing*, 27(8):667–687, 2013.
- [6] A. Ghosh, M. Abdalmoaty, S. Chatterjee, and H. Hjalmarsson. DeepBayes—An estimator for parameter estimation in stochastic nonlinear dynamical models. *Automatica*, 159:111327, 2024.
- [7] W. Greene. *Econometric analysis*. Prentice Hall, 2003.
- [8] M. Grieves and J. Vickers. Digital twin: Mitigating unpredictable, undesirable emergent behavior in complex systems. *Transdisciplinary perspectives on complex systems: New findings and approaches*, pages 85–113, 2017.
- [9] W. Kritzinger, M. Karner, G. Traar, J. Henjes, and W. Sihm. Digital twin in manufacturing: A categorical literature review and classification. *IFAC-PapersOnline*, 51(11):1016–1022, 2018.
- [10] B. Lakshminarayanan and C. R. Rojas. On asymptotic analysis of the two-stage approach: Towards data-driven parameter estimation. *arXiv preprint arXiv:2508.18201*, 2025.
- [11] L. Ljung. *System Identification: Theory for the User, 2nd Ed.* Prentice Hall, 1999.
- [12] K. Niu, M. Zhou, C. T. Abdallah, and M. Hayajneh. Deep transfer learning for system identification using long short-term memory neural networks. *arXiv preprint arXiv:2204.03125*, 2022.
- [13] S. J. Pan and Q. Yang. A survey on transfer learning. *IEEE Transactions on knowledge and data engineering*, 22(10):1345–1359, 2009.
- [14] D. Piga, M. Rufolo, G. Maroni, M. Mejari, and M. Forgione. Synthetic data generation for system identification: leveraging knowledge transfer from similar systems. In *2024 IEEE 63rd Conference on Decision and Control (CDC)*, pages 6383–6388. IEEE, 2024.
- [15] E. VanDerHorn and S. Mahadevan. Digital twin: Generalization, characterization and implementation. *Decision support systems*, 145:113524, 2021.
- [16] A. Wald. Tests of statistical hypotheses concerning several parameters when the number of observations is large. *Transactions of the American Mathematical society*, 54(3):426–482, 1943.
- [17] E. Wan and A. Nelson. Dual extended kalman filter methods. *Kalman filtering and neural networks*, pages 123–173, 2001.
- [18] L. Wasserman. *All of statistics: a concise course in statistical inference*. Springer Science & Business Media, 2013.
- [19] T. Wigren and J. Schoukens. Three free data sets for development and benchmarking in nonlinear system identification. In *2013 European control conference (ECC)*, pages 2933–2938. IEEE, 2013.
- [20] J. Yosinski, J. Clune, Y. Bengio, and H. Lipson. How transferable are features in deep neural networks? *Advances in neural information processing systems*, 27, 2014.